EUROPEAN ORGANIZATION FOR NUCLEAR RESEARCH

CERN-EP/87-35
February 18th, 1987

COMPARISON OF MULTIPLICITY DISTRIBUTIONS TO THE NEGATIVE BINOMIAL DISTRIBUTION IN MUON–PROTON SCATTERING

The European Muon Collaboration

Aachen[1], CERN[2], DESY (Hamburg)[3], Freiburg[4], Hamburg (University)[5], Kiel[6], LAL (Orsay)[7], Lancaster[8], LAPP (Annecy)[9], Liverpool[10], Marseille[11], Mons[12], MPI (München)[13], Oxford[14], RAL (Chilton)[15], Sheffield[16], Torino[17], Uppsala[18], Warsaw[19], Wuppertal[20]

M.Arneodo[17], A.Arvidson[18], J.J.Aubert[11], B.Badełek[19A], J.Beaufays[2], C.P.Bee[8B], C.Benchouk[11], G.Berghoff[1], I.Bird[8C], D.Blum[7], E.Böhm[6], X.de Bouard[9], F.W.Brasse[3], H.Braun[20], C.Broll[9†], S.Brown[10D], H.Brück[20E], H.Calen[18], J.S.Chima[15F], J.Ciborowski[19A], R.Clifft[15], G.Coignet[9], F.Combley[16], J.Coughlan[8G], G.D'Agostini[11], S.Dahlgren[18], F.Dengler[13], I.Derado[13], T.Dreyer[4], J.Drees[20], M.Düren[1], V.Eckardt[13], A.Edwards[20H], M.Edwards[15], T.Ernst[4], G.Eszes[9I], J.Favier[9], M.I.Ferrero[17], J.Figiel[5J], W.Flauger[3], J.Foster[16K], J.Ftáčnik[13], E.Gabathuler[10], J.Gajewski[5], R.Gamet[10], J.Gayler[3], N.Geddes[14G], P.Grafström[18], F.Grard[12], J.Haas[4], E.Hagberg[18], F.J.Hasert[1L], P.Hayman[10], P.Heusse[7], M.Jaffré[7], A.Jacholkowska[2], F.Janata[5], G.Jancsó[13I], A.S.Johnson[14M], E.M.Kabuss[4], G.Kellner[2], V.Korbel[3], J.Krüger[20E], S.Kullander[18], U.Landgraf[4], D.Lanske[1], J.Loken[14], K.Long[14N], M.Maire[9], P.Malecki[13J], A.Manz[13], S.Maselli[13], W.Mohr[4], F.Montanet[11], H.E.Montgomery[2O], E.Nagy[9I], J.Nassalski[19P], P.R.Norton[15], F.G.Oakham[15Q], A.M.Osborne[2], C.Pascaud[7], B.Pawlik[13J], P.Payre[11], C.Peroni[17], H.Peschel[20], H.Pessard[9], J.Pettinghale[10], B.Pietrzyk[11], U.Pietrzyk[20], B.Pönsgen[5], M.Pötsch[20], P.Renton[14], P.Ribarics[13I], K.Rith[4C], E.Rondio[19C], A.Sandacz[19P], M.Scheer[1], A.Schlagböhmer[4], H.Schiemann[5], N.Schmitz[13], M.Schneegans[9], A.Schneider[20], M.Scholz[1], T.Schröder[4], K.Schultze[1], T.Sloan[8], H.E.Stier[4], M.Studt[5], G.N.Taylor[14], J.M.Thénard[9], J.C.Thompson[15], A.de la Torre[5R], J.Toth[9I], L.Urban[1], L.Urban[9I], W.Wallucks[4], M.Whalley[16S], S.Wheeler[16], W.S.C.Williams[14], S.J.Wimpenny[10N], R.Windmolders[12] and G.Wolf[13]

(Submitted to Zeitschrift für Physik C)

1. *III Physikalisches Institut A, Physikzentrum, RWTH, D-5100 Aachen, Fed. Rep. Germany*
2. *CERN, CH-1211 Geneva 23, Switzerland*
3. *DESY, Notkestr. 85, D-2000 Hamburg 52, Fed. Rep. Germany*
4. *Fakultät für Physik, Universität Freiburg, Hermann – Herder Strasse 3, D-7800 Freiburg, Fed.Rep. Germany*
5. *II Institut für Experimentalphysik, Universität Hamburg, Luruper Chaussee 149, D-2000 Hamburg 50, Fed. Rep. Germany*
6. *Institut für Kernphysik, Universität Kiel, Olshausenstr. 40–60, D-2300 Kiel, Fed. Rep. Germany*
7. *Laboratoire de l'Accélérateur Linéare (LAL), Université de Paris-Sud, Bâtiment 200, F-91405 Orsay Cedex, France*
8. *Department of Physics, University of Lancaster, Bailrigg, Lancaster LA1 4YB, UK*
9. *Laboratoire d'Annecy-le-Vieux de Physique des Particules, B.P. 909, F-74019 Annecy-le-Vieux Cedex, France*
10. *Oliver Lodge Laboratory, Department of Physics, University of Liverpool, Oxford St., P.O. Box 147, Liverpool L69 3BX, UK*
11. *Centre de Physique de Particules, Faculté de Sciences de Luminy, Case 907, 70, route Léon Lachamp, F-13288 Marseille Cedex 9, France*
12. *Faculté des Sciences, Université de l'Etat à Mons, Avenue Maistriau 19, B-7000 Mons, Belgium*
13. *Max Planck Institut für Physik und Astrophysik, Föhringer Ring 6, Postfach 401212, D-8000 München 40, Fed. Rep. Germany*
14. *Nuclear Physics Laboratory, University of Oxford, Keble Road, Oxford OX1 3RH, UK*
15. *Rutherford and Appleton Laboratory, Chilton, Didcot OX11 0QX, UK*
16. *Department of Physics, University of Sheffield, The Hick's Building, Sheffield S3 7RH, UK*
17. *Instituto di Fisica, Università di Torino, Corso M. d'Azeglio 46, I-10125 Torino, Italy*
18. *Gustav Werners Institut, University of Uppsala, P.O. Box 531, S-75121 Uppsala, Sweden*
19. *Institute of Experimental Physics, University of Warsaw and Institute for Nuclear Studies, Hoża 69, PL-00-681 Warsaw, Poland*
20. *Fachbereich Physik, Universität Wuppertal, Gauss Strasse 20, Postfach 100 127, D-5600 Wuppertal, Fed. Rep. Germany*

A. *University of Warsaw, Poland.*
B. *Now at University of Liverpool, UK.*
C. *Now at MPI für Kernphysik, Heidelberg, Fed. Rep. Germany.*
D. *Now at TESA S.A., Renens, Switzerland.*
E. *Now at DESY, Hamburg, Fed. Rep. Germany.*
F. *Now at British Telecom, Ipswich, England.*
G. *Now at RAL, Chilton, Didcot, UK.*
H. *Now at Jet, Joint Undertaking, Abington, UK.*
I. *Permanent address: Central Research Institute for Physics of the Hungarian Academy of Science, Budapest, Hungary.*
J. *Permanent address: Institute of Nuclear Physics, Kraków, Poland.*
K. *Now at University of Manchester, England.*
L. *Now at Krupp Atlas Elektronic GmbH, Bremen, Fed. Rep. Germany.*
M. *Now at SLAC, Stanford, California, U.S.A.*
N. *Now at CERN, Geneva, Switzerland.*
O. *Now at FNAL, Batavia, Illinois, U.S.A.*
P. *Institute for Nuclear Studies, Warsaw, Poland.*
Q. *Now at NRC, Ottawa, Canada.*
R. *Now at Universidad Nacional, Mar del Plata, Argentina.*
S. *Now at University of Durham, UK.*
†. *Deceased*

ABSTRACT

The multiplicity distributions of charged hadrons produced in the deep inelastic muon–proton scattering at 280 GeV are analysed in various rapidity intervals, as a function of the total hadronic centre of mass energy W ranging from 4 to 20 GeV. Multiplicity distributions for the backward and forward hemispheres are also analysed separately. The data can be well parameterized by binomial distributions, extending their range of applicability to the case of lepton – proton scattering. The energy and the rapidity dependence of the parameters is presented and a smooth transition from the negative binomial distribution via poissonian to the ordinary binomial is observed.

1. Introduction

Several measurements of multiplicity distributions $P(n)$ have been collected so far in experiments with hadron and lepton beams at centre–of–mass (cm) energies up to 900 GeV [1–4]. In this context the question has been raised as to the relationship between the form of the multiplicity distributions and the mechanisms responsible for multiparticle production. Several phenomenological rules have been proposed to parameterize multiplicity distributions [1, 5, 6] and to describe their energy dependence. In a recent analysis [1] the UA5 collaboration has shown that the charged particle multiplicity distribution follows the negative binomial distribution (NBD). In addition it was shown that the multiplicities, not only of all charged particles produced in full phase space but also of those produced in limited pseudorapidity regions, are remarkably well described by the NBD, i.e. by a distribution of the form

$$P(n;k,\bar{n}) = \frac{k(k+1)\dots(k+n-1)}{n!}\Big(\frac{\bar{n}}{\bar{n}+k}\Big)^n\Big(\frac{k}{\bar{n}+k}\Big)^k \qquad (1)$$

where k and $\bar{n}$ are free parameters.

The average multiplicity $<n>$ and the dispersion D of the NBD are related to the two parameters as follows:

$$< n >= \bar{n} \quad , \quad D^2 = \bar{n} + \frac{\bar{n}^2}{k} \ . \qquad (2)$$

In addition to the multiplicity distribution $P(n)$ the KNO distribution [5], i.e. the distribution $\Psi(z) = <n> \cdot P(n)$ of the reduced multiplicity $z = \frac{n}{<n>}$, is often used. The average value $<z>$ and the dispersion D_z of binomial distributions in terms of the z variable are:

$$< z >= 1 \quad , \quad D_z^2 = \frac{1}{\bar{n}} + \frac{1}{k} \ . \tag{3}$$

The original observations of the UA5 collaboration have recently been followed by similar results obtained in several other experiments. Charged multiplicity distributions, measured in various rapidity intervals, for hadron–hadron collisions [7], for e^+e^- annihilation [2], and even for proton–nucleus interactions [8] are well described by the distribution of type (1).

These experimental findings led to several investigations as to the physical interpretation of the observed empirical law. In recent papers [9, 10], some general mechanisms of particle production, namely stimulated emission and cascade type production via independent clans (types of clusters), were discussed. It was also shown that the NBD rule for multiplicity distributions may hold for certain jet fragmentation processes in QCD [11, 12], for a model with a bremsstrahlung analogy [13], for the "minimal" cluster model [14] and, to some extent, for the dual parton model [15]. Correspondingly, the dependence of the NBD parameters on energy and rapidity span has several possible interpretations. It can be associated with the characteristics of particle production in hard (e^+e^- , lepton–hadron) and soft (hadron–hadron) collisions [3, 16], with particular properties of clusters [9], with a phase-transition like behaviour resulting from the excitation of the quark-gluon plasma in hadron–hadron collisions [17] or with the effect of energy–momentum conservation [13].

One should however be aware that, despite this successful parameterization, descriptions alternative to the NBD, and of an equally good statistical merit, have been suggested [3, 18, 19]. In particular, it was argued recently [19] that the problematic physical interpretation of the very large and rapidly varying parameter k may be avoided when one considers a generalization of the NBD, namely a three – parameter distribution describing a partially coherent emission from k sources [20]. Before it is possible to draw more definite conclusions about the

proposed physical interpretations just mentioned, more experimental results of high precision for various reactions and energies are needed.

In the present paper multiplicity distributions of charged hadrons produced in deep inelastic muon–proton collisions at 280 GeV are analysed for various rapidity intervals centred around a rapidity of zero in the virtual photon – proton cm system. Furthermore, our previous studies [21, 22] indicate considerable differences between hadronic final states produced in the forward and in the backward hemisphere. Therefore, an analysis of multiplicities was also performed for each hemisphere separately.

In the following section a brief description of the experimental data and of the analysis procedure is given. The results are presented and discussed in section 3, followed by concluding remarks.

2. Experimental data and analysis

The data were taken by the European Muon Collaboration in the NA9 experiment at the 280 GeV muon M2 beam line from the CERN SPS. The detector consisted of a vertex spectrometer and a forward spectrometer, which were used to detect and measure all charged particles of momenta bigger than 0.2 GeV/c. It was described in detail in an earlier publication [23]. There, and in references [21, 24, 25], details can be found of the methods used for event reconstruction and particle identification with an extensive system of Cherenkov and time of flight counters, and of the procedure for the various corrections applied to the data. In order to restrict the event sample to regions where the corrections for event acceptance, smearing effects from the resolution of the apparatus and radiative corrections are relatively small ($\leq$10%), the following selection criteria were applied:

$$4GeV^2 < Q^2 < 200GeV^2$$

$$20GeV < \nu < 260GeV$$

$$4GeV < W < 20GeV$$

$$E_{\mu'} > 20GeV, \qquad \frac{\nu}{E_\mu} < 0.9, \qquad \Theta_{\mu'} > 0.75^o$$

In this list $(-Q^2)$ is the square of the four–momentum transfer between the in-

cident muon and the target proton, $\nu = E_\mu - E_{\mu'}$ is the corresponding energy transfer in the laboratory system, E_μ and $E_{\mu'}$ are the energy of the incident and the scattered muon, respectively, in the laboratory system, W is the cms total energy of the final state hadrons and $\Theta_{\mu'}$ is the laboratory angle between the incident and scattered muon.

The number of events remaining after the cuts was 25569. About 50 % of the charged particles in these events were identified by the apparatus. The pion mass was assigned to the remaining particles. The events were subdivided into eight samples according to the cms energy W . The average value of W for each sample and the corresponding number of events are given in Table 1.

Multiplicity distributions have been determined in the full phase space as well as in restricted rapidity intervals. The observed multiplicity distributions were corrected by means of a matrix unfolding technique:

$$P^c(n) = \sum_m C_{nm} P^o(m) \tag{4}$$

where $P^o(m)$ is the observed multiplicity distribution and $P^c(n)$ is the corrected multiplicity distribution. The matrix C_{nm} was determined from a detailed Monte Carlo simulation of the experiment, separately for each rapidity and W interval. C_{nm} is the probability that an event with n charged particles has m of them detected.

The corrected multiplicity distributions of particles produced in the selected rapidity windows were fitted to the two-parameter binomial distribution, eq.(1). This distribution reduces to the Poisson distribution as $k \to \infty$. For negative values of the parameter k the distribution (1) becomes an ordinary binomial distribution, which is narrower than the Poissonian (see eq.(2)). When multiplicity distributions are close to the Poisson limit ($\frac{1}{k} = 0$), i.e. for large positive or large negative values of k, it is appropriate to use $\bar{n}$ and $1/k$ as the pair of fitted parameters.

The fitting algorithm allowed for a smooth transition from positive to negative values of the parameter $1/k$. It is easy to show that the form of the ordinary binomial distribution following from the parameterization of eq. (1) is useful only when the values of the parameter k are considerably greater than $\bar{n}$. This is always the case here.

3. Results

3.1. Multiplicity distributions of all charged particles

For the eight W intervals listed in Table 1 multiplicity distributions of charged hadrons were determined for various widths of the cms rapidity interval of the produced particles. The rapidity intervals were chosen to be of width $2 \cdot \Delta y$, with Δy increasing in steps of 0.5 units from the smallest value of 0.5, centred symmetrically around zero rapidity in the virtual photon – proton cm system.

The effect of charge conservation on charged hadron multiplicity distributions requires special treatment. For the full phase space, the charged multiplicity is odd in the case of muon - proton scattering. For limited rapidity intervals the multiplicity distribution shows clear even/odd prong fluctuations. For smaller, more resticted rapidity windows, with the width depending on the cms energy, these fluctuations disappear and both even and odd prongs follow the same distribution. For such small windows, fits to the multiplicity distributions were performed using both odd and even prongs. For the less restricted intervals, only the odd prongs were taken into consideration.

The results of the fits are summarized in Table 2, where for each W interval and rapidity interval of $2 \cdot \Delta y$, the fitted values of parameters $\bar{n}$ and $1/k$ and the ratio χ^2/N_{df} characterizing the fit quality are given. The values for the widest rapidity interval quoted for a given energy may be regarded as representing the results for the full phase space available at this energy; no significant change of the parameters was observed when the rapidity window was widened beyond this value. The errors quoted on the parameters are statistical only. The main source of systematic errors is the correction technique used for the multiplicity distributions, eq.(4). It fully relies on the accuracy of the Monte Carlo simulation of this experiment. An estimate of the systematic errors indicates that the error on both $\bar{n}$ and $1/k$ is of the same order as the corresponding statistical error.

The quality of the fits is satisfactory for the majority of the distributions. This shows that the remarkably good description of multiplicity distributions by the NBD as observed for various types of reactions applies also to deep inelastic muon – proton scattering, provided one considers the whole family of binomial

distributions, including the Poisson and ordinary binomial distributions.

As an example, Fig. 1 shows the distributions and the fits for the highest energy interval. In the figure one can also observe, between the distributions for $\Delta y = 1.5$ and $\Delta y = 2$, the transition from fitting all prongs to fitting only odd prongs. (Sometimes, because of the logarithmic scale, the last points with the lowest values and the largest errors are not shown. However, all the non–zero values were used in the fits.)

3.2. MULTIPLICITIES OF CHARGED PARTICLES PRODUCED IN THE FORWARD AND IN BACKWARD HEMISPHERES

The charged multiplicity distributions have also been analysed separately in the forward and backward hemispheres in a way analogous to that described in the previous section. In the framework of the quark parton model the forward multiplicity is related to the fragmentation of the scattered quark while the backward multiplicity results mostly from the remnant target fragmentation. It has been observed previously that for lepton – hadron reactions, the forward and backward multiplicity distributions differ considerably and that the multiplicities in the two hemispheres are only weakly correlated [4, 21].

The forward and backward multiplicity distributions were fitted separately for each of the eight W intervals listed in Table 1, and for each selected rapidity interval. Intervals of width Δy increasing from 0.5 in steps of 0.5 rapidity units were considered, extending from the cms rapidity $y = 0$ to positive values for the forward hemisphere and to negative values for the backward hemisphere. The fitted parameters $\bar{n}$ and $1/k$ are summarized in Table 3 for the forward and in Table 4 for the backward hemisphere, where also the χ^2 and the number of degrees of freedom N_{df} are given for each fit. As an example, Figs. 2a and 2b show the multiplicity distributions and the fits for the highest W interval for the forward and for the backward hemisphere, respectively.

The analysis shows that these distributions are also well parameterized by binomial distributions. The differences of the backward and forward multiplicities and their energy and rapidity dependences can thus be described in terms of the parameters $\bar{n}$ and $1/k$ of binomial distributions.

3.3. ENERGY DEPENDENCE OF THE PARAMETERS $\bar{n}$ AND $1/k$

The energy dependence of the parameter $\bar{n}$, representing the mean multiplicity, is shown in Fig. 3a for several rapidity intervals $2 \cdot \Delta y$, centered around zero cms rapidity (see also Table 2). A similar energy dependence of $\bar{n}$ is observed for multiplicity distributions in the forward and in the backward hemispheres separately (Tables 3 and 4). The $\bar{n}$ increases very slowly with energy in the small rapidity intervals in the central rapidity region, which is consistent with our previous observation [26] that the density at zero rapidity is approximately energy independent and the width of the rapidity distribution increases logarithmically. The energy dependence shows up more clearly with increasing width of the rapidity interval. For the larger rapidity intervals $\bar{n}$ shows an increase which slows down with the increasing W.

The weak energy dependence of $\bar{n}$, especially for the smallest rapidity intervals, concurs with the clear increase with energy of the parameter $1/k$, observed for all rapidity intervals. This is illustrated for some of the intervals $2 \cdot \Delta y$ in Fig.3b. According to eq. (3), the interplay of the energy dependences of the two terms $1/\bar{n}$ and $1/k$ implies a clear broadening of the KNO multiplicity distributions in the central rapidity region with the increasing W. The opposite effect was recently predicted for e^+e^- annihilation [27]. Such a clear violation of KNO scaling in the central region has not been observed before. To show this effect independently of the NBD fits we present in Table 5, in addition to $<n>$ and D^2, the skewness γ_3 and the kurtosis γ_4 as functions of W, determined from the multiplicity distributions for the rapidity interval $2 \cdot \Delta y = 2$. The skewness and the kurtosis are given by

$$\gamma_3 = \frac{\mu_3}{{\mu_2}^{3/2}} \quad , \quad \gamma_4 = \frac{\mu_4}{{\mu_2}^2} - 3 \tag{5}$$

where

$$\mu_q = < (n - < n >)^q > \quad . \tag{6}$$

These quantities γ_3 and γ_4 show a clear increase with W in the central region whereas they should be constant if KNO scaling holds exactly.

For the full phase space multiplicity distributions the energy dependences of the two terms $1/\bar{n}$ and $1/k$ almost compensate each other in the W range covered

by this experiment. According to eq.(3) this implies (approximate) KNO scaling in this W range. If the observed energy dependences of $1/\bar{n}$ and $1/k$ continue towards higher W, then KNO scaling would be considerably violated there, as observed for hadron – hadron collisions [1].

We now compare the energy dependence of $1/k$ observed in this experiment in the full rapidity range with various reactions for which the multiplicity distributions for the full rapidity ranges are given. For pp and $\bar{p}p$ collisions $1/k$ was found by the UA5 collaboration [1] to increase approximately linearly with the logarithm of the cms energy over the range of 10 to 900 GeV. A similar regularity was recently observed [3] for e^+e^- annihilation. The resulting linear fits are shown in Fig. 4 by the dashed line for pp and $\bar{p}p$ scattering and by the solid line for e^+e^- annihilation. In e^+e^- annihilation lower $1/k$ values are found with a somewhat slower increase with energy. In the same figure we also show the points for meson - proton (Mp) collisions from ref. [3], and our data points from Table 2. Both the Mp and μ^+p points fall between the lines for pp-$\bar{p}p$ and e^+e^-. Furthermore, the μ^+p points tend to be systematically somewhat lower than the Mp points and closer to the e^+e^- line than to the pp-$\bar{p}p$ line. In order to investigate further this similarity between $1/k$ for μ^+p and e^+e^- scattering, we show in Fig. 5b the energy dependence of $1/k$ for μ^+p scattering separately for the full forward and backward hemispheres. The solid line shows $1/k$ for one hemisphere of e^+e^- annihilation as derived from $1/k$ for both e^+e^- hemispheres with the assumption that the two hemispheres are uncorrelated. The data points for the forward μ^+p hemisphere are seen to fall close to the values for one e^+e^- hemisphere. This observation supports the concept of universality of quark fragmentation.

Comparing the forward ($y > 0$) and backward ($y < 0$) μ^+p multiplicity distributions one observes that $\bar{n}$ is smaller in the backward than in the forward hemisphere (Fig. 5a) whereas the width D_z of the KNO distribution is smaller in the forward than in the backward hemisphere (eq.(3) and Fig. 5). In order to examine whether these differences may be due to the somewhat arbitrary choice of $y = 0$ as the boundary between the two hemispheres, we have shifted this boundary to $y = 0.25$ such that the two $\bar{n}$ values become more similar. This is seen in Fig. 6a which shows the W dependence of the fitted $\bar{n}$ for the two rapidity ranges $y > 0.25$ ("forward") and $y < 0.25$ ("backward"). However the forward

– backward difference for the second parameter $1/k$, becomes even larger for the new choice of the boundary (Fig. 6b) than for the boundary $y = 0$ (Fig. 5b) (although the slopes of the W dependence are now rather similar). This indicates that there is a genuine difference between the multiplicity distributions for quark and target remnant fragmentation.

3.4. RAPIDITY DEPENDENCE OF THE PARAMETER $1/k$ AND THE FORWARD – BACKWARD ASYMMETRY

Another aspect of the difference between forward and backward multiplicities discussed above may be deduced from the dependence of the parameter $1/k$ on the rapidity interval Δy. Fig. 7 illustrates this dependence for the backward and the forward hemisphere, for various W intervals (see also Table 3 and 4). The fast decrease of $1/k$ with increasing Δy in the forward hemisphere contrasts with the development of a maximum at small Δy in the backward hemisphere. For the highest W interval a broad maximum extends over about two units in rapidity.

The parameter $1/k$ of the multiplicity distribution of particles produced in a certain rapidity interval is related [9] to the two – particle correlation in this interval by

$$\frac{1}{k} = \frac{1}{\bar{n}^2} \int \int C_2(y_1, y_2) dy_1 dy_2 \tag{7}$$

where the correlation function $C_2(y_1, y_2)$ is given by the two-particle density $\rho_2(y_1, y_2)$ and single particle densities $\rho_1(y)$:

$$C_2(y_1, y_2) = \rho_2(y_1, y_2) - \rho_1(y_1) \cdot \rho_1(y_2) \tag{8}$$

One can conclude from eq. (7) that the clear difference of the parameter $1/k$ in the forward and backward hemispheres indicates (particularly for higher W) the existence of short and medium range positive two – particle rapidity correlations, which are considerably stronger in the backward hemisphere than in the forward hemisphere.

In a recent analysis of the charged particle rapidity correlations based on the data from this experiment [28] it has been found that the two – particle rapidity correlations are indeed stronger in the backward than in the forward hemisphere. This is illustrated in Fig. 8, which shows the two – particle correlation

function $C_2(y_1, y_2)$ for three intervals of y_2 selected in the backward and forward hemispheres and in the central rapidity region, for events in the energy range $12 < W < 20$ GeV. It has also been found that the difference between the forward and backward hemispheres in the correlation strength increases with increasing W. These results agree qualitatively with our observations.

4. Summary and conclusions

We have parametrized multiplicity distributions of charged hadrons produced in the deep inelastic muon – proton scattering at 280 GeV by binomial distributions. The multiplicity distributions, corresponding to various energies W and rapidity intervals Δy , have been fitted to the two parameter formula of eq. (1). The quality of the majority of the fits is good. This confirms that the negative binomial distribution (NBD) represents an effective way of parameterizing multiplicity distributions. Our analysis shows, that the "NBD law" includes the whole family of binomial distributions with a smooth transitions, via the rapidity and energy dependence of the parameters, from negative binomial through Poissonian to ordinary binomial distributions.

The satisfactory description by binomial distributions means that a study of multiplicity distributions can be made in terms of the parameters $\bar{n}$ and $1/k$. The energy behaviour of $1/k$ was compared for various reactions in connection with the concept of "jet universality" and found to be very similar for the forward μp hemisphere and one e^+e^- hemisphere.

The observed differences between the forward and the backward multiplicities expressed in terms of the rapidity dependence of the NBD parameters, indicate that there are stronger short and medium range two – particle correlations in the backward than in the forward hemisphere.

5. Acknowledgements

We are grateful to Krzysztof Fiałkowski and Leon Van Hove for useful discussions and correspondence. Thanks are due to Andrzej Białas for suggesting this investigation and for helpful remarks. Furthermore we would like to thank all people in the various laboratories who contributed to the construction, operation and analysis of this experiment. The support of the CERN staff in operating the SPS, muon beam and computer facilities is gratefully acknowledged.

REFERENCES

[1] G.J.Alner et al., *Phys. Lett.* **160 B** (1985) 193.
G.J.Alner et al., *Phys. Lett.* **160 B** (1985) 199.
G.J.Alner et al., *Phys. Lett.* **167 B** (1986) 476.

[2] M. Derrick et al., *Phys. Lett.* **168 B** (1986) 299.

[3] M. Adamus et al., *Z. Phys. C – Particles and Fields* **32** (1986) 475.
See also refs. 29 – 31 therein.

[4] D. Ziemińska et al., *Phys. Rev.* **D 27** (1983) 47.
H. Grässler et al., *Nucl. Phys.* **B 223** (1983) 269.

[5] Z. Koba, H.B. Nielsen and P. Olesen, *Nucl. Phys.* **B 40** (1972) 317.

[6] P. Slattery, *Phys. Rev. Lett.* **29** (1972) 1624.
O. Czyżewski and K.Rybicki, *Nucl. Phys.* **B 47** (1972) 633.
A.J.Buras, J.Dias de Deus and R.Møller, *Phys. Lett.* **47 B** (1973) 251.
D. Levy, *Nucl. Phys.* **B 59** (1973) 583.

[7] M. Adamus et al., *Phys. Lett.* **177 B** (1986) 239.

[8] F. Dengler et al., *Z. Phys. C – Particles and Fields* **33** (1986) 187.

[9] A. Giovannini and L. Van Hove, *Z. Phys. C – Particles and Fields* **30** (1986) 391.

[10] L. Van Hove and A. Giovannini, Negative binomial multiplicity distributions, a new empirical law for high energy collisions. University of Torino preprint. DFTT 11/86. May 1986.

[11] A. Giovannini, *Nucl. Phys.* **B 161** (1979) 429.

[12] E.D. Malaza and B.R. Webber, *Nucl. Phys.* **B 267** (1986) 702.

[13] A.Białas, I.Derado and L.Stodolsky, *Phys. Lett.* **156 B** (1985) 421.

[14] K.Fiałkowski, *Phys. Lett.* **173 B** (1986) 197.

[15] A. Capella, A. Staar and J. Tran Thanh Van, *Phys. Rev.* **D 32** (1985) 2933
A.V. Batunin and A.N. Tolstenkov *Yad. Fiz.* **42** (1985) 970.

[16] W. Kittel, Brief review of jet universality. Review talk at XXIth Rencontre de Moriond, Les Arcs, 16–22 March 1986.

[17] P. Carruthers, E.M. Friedlander and R.M. Weiner, *Physica* **23 D** (1986) 138.

[18] Wei–qin Chao, Ta–chung Meng and Ji–cai Pan, *Phys. Lett.* **176 B** (1986) 211.

[19] P. Carruthers, Proc. XXI Rencontre de Moriond, Les Arcs, France, Vol.2, p.229(1986).
P. Carruthers and C.C. Shih, $e^+ - e^-$ hadronic multiplicity distributions. Los Alamos National Laboratory preprint. LA–UR–86–2705. June 1986. submitted to Phys. Rev. D.

[20] P. Carruthers and C.C. Shih, *Phys. Lett.* **137 B** (1984) 425.

[21] EMC, M. Arneodo et al., *Nucl. Phys.* **B 258** (1985) 249.

[22] EMC, M.Arneodo et al., *Phys. Lett.* **149 B** (1984) 415.

[23] EMC, J.P. Albanese et al., *Nucl. Instr. and Meth.* **212** (1983) 111.

[24] EMC, M. Arneodo et al., *Nucl. Phys.* **B 264** (1986) 739.

[25] EMC, M. Arneodo et al., Comparison between hadronic final states produced in μp and e^+e^- interactions. CERN – EP/86 – 119, September 1986

[26] EMC, M.Arneodo et al., *Z. Phys. C – Particles and Fields* **31** (1986) 1.

[27] A.Białas and F.Hayot, *Phys. Rev.* **D 33** (1986) 39.

[28] J. Krüger, Ph. D. Thesis, Wuppertal (1985), WU B–DI 85–4.

Tab. 1: Number of events N and the average hadronic energy $< W >$ in the selected energy intervals.

W (GeV)	4 ÷ 6	6 ÷ 8	8 ÷ 10	10 ÷ 12	12 ÷ 14	14 ÷ 16	16 ÷ 18	18 ÷ 20
N	1304	2453	3044	3193	3305	3551	3984	4735
<W> (GeV)	5.2	7.0	9.0	11.0	13.0	15.0	17.0	19.0

Tab. 2: Parameters of binomial distributions, fitted to the measured charged multiplicity distributions, followed by the χ^2 and the number of degrees of freedom for various rapidity intervals $2 \cdot \Delta y$ centred around $y = 0$, for various intervals of the total hadronic energy W.

Δy	$\bar{n}$	$1/k$	χ^2/N_{df}	Δy	$\bar{n}$	$1/k$	χ^2/N_{df}
W = 4 ÷ 6 GeV				W = 6 ÷ 8 GeV			
0.5	1.45±0.03	0.093±0.025	2.0/6	0.5	1.47±0.02	0.068±0.016	3.7/7
1.0	2.80±0.05	0.061±0.022	0.7/3	1.0	2.85±0.03	0.055±0.009	16.5/10
1.5	3.82±0.05	-0.032±0.009	4.0/3	1.5	4.12±0.05	0.029±0.008	27.5/4
2.0	4.06±0.04	-0.054±0.006	2.9/4	2.0	4.84±0.04	-0.026±0.005	3.2/4
2.5	4.08±0.04	-0.058±0.005	4.0/4	2.5	4.89±0.03	-0.034±0.004	3.0/4
W = 8 ÷ 10 GeV				W = 10 ÷ 12 GeV			
0.5	1.50±0.02	0.120±0.016	2.8/8	0.5	1.53±0.02	0.138±0.016	5.6/8
1.0	2.94±0.03	0.094±0.009	2.6/10	1.0	3.03±0.03	0.097±0.008	13.0/11
1.5	4.17±0.03	0.049±0.005	30.1/13	1.5	4.34±0.03	0.062±0.005	10.6/14
2.0	5.31±0.04	0.005±0.005	15.0/5	2.0	5.55±0.04	0.026±0.005	10.3/6
2.5	5.56±0.03	-0.016±0.003	7.0/6	2.5	6.07±0.04	-0.006±0.003	5.4/6
3.0	5.55±0.03	-0.018±0.003	5.5/6	3.0	6.09±0.03	-0.013±0.003	6.6/6
W = 12 ÷ 14 GeV				W = 14 ÷ 16 GeV			
0.5	1.52±0.02	0.174±0.016	0.7/8	0.5	1.52±0.02	0.136±0.015	2.8/8
1.0	3.01±0.03	0.119±0.008	6.5/12	1.0	3.02±0.03	0.123±0.009	4.0/12
1.5	4.37±0.03	0.084±0.006	10.8/14	1.5	4.38±0.03	0.086±0.005	16.5/15
2.0	5.66±0.05	0.054±0.006	14.2/7	2.0	5.60±0.05	0.073±0.006	6.0/7
2.5	6.46±0.04	0.004±0.003	12.1/7	2.5	6.71±0.04	0.022±0.004	11.2/7
3.0	6.51±0.03	-0.002±0.003	4.9/7	3.0	6.85±0.04	0.003±0.003	1.7/7
W = 16 ÷ 18 GeV				W = 18 ÷ 20 GeV			
0.5	1.54±0.02	0.186±0.015	3.5/9	0.5	1.57±0.02	0.212±0.014	0.8/10
1.0	3.06±0.02	0.137±0.008	3.3/12	1.0	3.12±0.02	0.163±0.008	7.9/13
1.5	4.53±0.03	0.105±0.006	3.1/15	1.5	4.56±0.03	0.127±0.005	12.2/17
2.0	5.78±0.05	0.073±0.005	9.9/9	2.0	5.75±0.05	0.104±0.006	11.2/8
2.5	6.94±0.05	0.033±0.004	23.7/9	2.5	7.00±0.05	0.061±0.004	35.3/9
3.0	7.25±0.04	0.010±0.003	2.5/9	3.0	7.51±0.04	0.025±0.003	4.1/9
3.5	7.20±0.03	0.007±0.002	2.8/9	3.5	7.48±0.03	0.017±0.002	9.8/9

Tab. 3: Same as Table 2 but for rapidity intervals Δy in the forward hemisphere, extending from $y = 0$ to positive values.

Δy	$\bar{n}$	$1/k$	χ^2/N_{df}	Δy	$\bar{n}$	$1/k$	χ^2/N_{df}
W = 4 ÷ 6 GeV				W = 6 ÷ 8 GeV			
0.5	0.69±0.02	0.081±0.069	2.5/4	0.5	0.74±0.02	0.091±0.049	3.0/4
1.0	1.31±0.03	0.038±0.035	5.1/6	1.0	1.48±0.03	0.047±0.020	5.9/7
1.5	1.80±0.03	-0.066±0.020	3.9/6	1.5	2.10±0.03	-0.013±0.013	5.6/7
2.0	2.03±0.03	-0.110±0.015	2.4/6	2.0	2.45±0.03	-0.051±0.010	6.8/7
2.5	2.10±0.03	-0.136±0.013	4.7/6	2.5	2.60±0.03	-0.081±0.009	6.8/7
W = 8 ÷ 10 GeV				W = 10 ÷ 12 GeV			
0.5	0.79±0.01	0.133±0.021	6.8/4	0.5	0.80±0.01	0.156±0.020	2.1/5
1.0	1.58±0.01	0.091±0.010	14.0/6	1.0	1.61±0.01	0.088±0.010	8.8/6
1.5	2.28±0.01	0.037±0.007	2.4/7	1.5	2.36±0.01	0.050±0.006	7.9/9
2.0	2.74±0.01	-0.018±0.005	6.9/7	2.0	2.90±0.01	-0.004±0.004	10.8/9
2.5	2.95±0.01	-0.050±0.004	3.3/7	2.5	3.17±0.02	-0.037±0.004	3.2/9
3.0	3.01±0.01	-0.062±0.004	14.1/7	3.0	3.26±0.01	-0.048±0.004	4.1/9
W = 12 ÷ 14 GeV				W = 14 ÷ 16 GeV			
0.5	0.80±0.01	0.162±0.019	6.6/4	0.5	0.78±0.01	0.116±0.019	5.4/5
1.0	1.64±0.01	0.130±0.010	9.1/7	1.0	1.62±0.01	0.113±0.010	4.1/8
1.5	2.43±0.01	0.085±0.006	15.5/8	1.5	2.42±0.01	0.074±0.006	9.0/10
2.0	3.06±0.02	0.021±0.004	3.6/10	2.0	3.07±0.02	0.029±0.004	6.9/10
2.5	3.42±0.02	-0.017±0.004	4.3/10	2.5	3.48±0.02	-0.012±0.004	3.8/10
3.0	3.55±0.02	-0.031±0.004	9.6/10	3.0	3.65±0.02	-0.032±0.003	9.5/10
W = 16 ÷ 18 GeV				W = 18 ÷ 20 GeV			
0.5	0.79±0.01	0.193±0.018	2.4/5	0.5	0.79±0.01	0.215±0.017	8.4/6
1.0	1.62±0.01	0.138±0.009	5.7/8	1.0	1.61±0.01	0.171±0.009	8.1/8
1.5	2.45±0.01	0.097±0.006	4.0/9	1.5	2.43±0.01	0.113±0.006	4.8/10
2.0	3.14±0.02	0.047±0.004	9.9/10	2.0	3.12±0.01	0.057±0.004	14.3/11
2.5	3.59±0.02	0.008±0.004	15.8/10	2.5	3.56±0.01	0.023±0.003	13.8/11
3.0	3.79±0.02	-0.014±0.003	10.3/11	3.0	3.85±0.02	-0.006±0.003	10.2/11
3.5	3.88±0.02	-0.026±0.003	17.6/11	3.5	3.96±0.01	-0.022±0.003	17.5/11

Tab. 4: Same as Table 2 but for rapidity intervals Δy in the backward hemisphere, extending from $y = 0$ to negative values.

Δy	$\bar{n}$	$1/k$	χ^2/N_{df}	Δy	$\bar{n}$	$1/k$	χ^2/N_{df}
W = 4 ÷ 6 GeV				W = 6 ÷ 8 GeV			
0.5	0.72±0.03	0.133±0.075	1.2/3	0.5	0.73±0.02	0.054±0.042	1.2/4
1.0	1.31±0.03	0.045±0.029	8.4/5	1.0	1.36±0.03	0.105±0.026	4.5/5
1.5	1.72±0.03	-0.065±0.019	4.6/5	1.5	1.81±0.03	0.034±0.014	29.6/6
2.0	1.83±0.03	-0.084±0.018	3.0/5	2.0	2.09±0.03	-0.045±0.011	11.3/7
2.5	1.85±0.03	-0.090±0.017	3.0/5	2.5	2.14±0.03	-0.052±0.010	12.0/7
W = 8 ÷ 10 GeV				W = 10 ÷ 12 GeV			
0.5	0.71±0.02	0.134±0.043	0.3/4	0.5	0.73±0.02	0.144±0.041	1.4/4
1.0	1.35±0.02	0.151±0.023	3.8/8	1.0	1.42±0.02	0.182±0.023	3.4/7
1.5	1.90±0.03	0.124±0.017	10.3/7	1.5	1.97±0.03	0.187±0.018	8.8/8
2.0	2.30±0.03	0.028±0.011	15.5/8	2.0	2.44±0.03	0.108±0.014	25.2/8
2.5	2.43±0.03	0.003±0.011	5.3/7	2.5	2.67±0.03	0.038±0.011	4.8/8
3.0	2.46±0.03	-0.002±0.010	5.6/7	3.0	2.71±0.03	0.034±0.011	6.2/8
W = 12 ÷ 14 GeV				W = 14 ÷ 16 GeV			
0.5	0.72±0.02	0.217±0.043	0.3/5	0.5	0.74±0.02	0.164±0.041	0.7/4
1.0	1.37±0.02	0.180±0.023	5.1/7	1.0	1.40±0.02	0.217±0.024	2.3/7
1.5	1.94±0.03	0.186±0.018	4.8/8	1.5	1.98±0.03	0.215±0.018	2.7/9
2.0	2.41±0.03	0.146±0.014	23.9/9	2.0	2.47±0.03	0.188±0.014	17.8/10
2.5	2.75±0.03	0.052±0.010	6.6/9	2.5	2.88±0.03	0.099±0.011	12.5/10
3.0	2.83±0.03	0.038±0.010	3.9/9	3.0	3.03±0.03	0.054±0.009	2.8/10
W = 16 ÷ 18 GeV				W = 18 ÷ 20 GeV			
0.5	0.75±0.01	0.200±0.036	1.4/5	0.5	0.77±0.01	0.209±0.034	0.3/5
1.0	1.45±0.02	0.215±0.022	1.3/8	1.0	1.49±0.02	0.243±0.021	10.8/8
1.5	2.07±0.03	0.210±0.017	3.3/9	1.5	2.13±0.03	0.268±0.017	10.1/9
2.0	2.58±0.03	0.201±0.014	14.9/9	2.0	2.66±0.03	0.244±0.014	16.5/11
2.5	3.02±0.03	0.116±0.011	29.2/10	2.5	3.14±0.03	0.165±0.011	31.8/11
3.0	3.24±0.03	0.054±0.008	6.4/10	3.0	3.43±0.03	0.070±0.007	16.2/13
3.5	3.28±0.03	0.048±0.008	6.8/10	3.5	3.49±0.03	0.060±0.007	10.2/13

Tab. 5: Average multiplicity <n>, dispersion D^2, skewness γ_3 and kurtosis γ_4 for multiplicity distributions of charged hadrons produced in the cms rapidity interval $-1.0 \leq y \leq +1.0$ as functions of cms energy W.

W (GeV)	<n>	D^2	γ_3	γ_4
4 – 6	2.69±0.05	3.04±0.12	1.05±0.22	0.19±0.45
6 – 8	2.85±0.04	3.31±0.10	1.27±0.19	0.40±0.40
8 – 10	2.94±0.03	3.72±0.11	1.50±0.19	0.61±0.37
10 – 12	3.03±0.04	3.94±0.11	1.63±0.19	0.71±0.38
12 – 14	3.01±0.04	4.09±0.12	1.63±0.19	0.67±0.39
14 – 16	3.02±0.03	4.13±0.12	1.74±0.20	0.91±0.42
16 – 18	3.07±0.03	4.39±0.12	1.86±0.21	1.02±0.43
18 – 20	3.12±0.03	4.69±0.12	1.92±0.20	1.02±0.41

FIGURE CAPTIONS

1. Charged multiplicity distributions for μp interactions for various cms rapidity intervals $2 \cdot \Delta y$ extending from $-\Delta y$ to $+\Delta y$ and for cms energies W in the range from 18 to 20 GeV. The histograms show the negative binomial distributions fitted to the data point The distribution for the widest interval is shown in the ordinary scale, each consecutive one is shifted down by a factor of ten.

2. Same as Fig. 1 but for rapidity intervals extending from $y = 0$ to (a) $+\Delta y$ in the forward hemisphere, and to (b) $-\Delta y$ in the backward hemisphere.

3. Values of the parameters of the negative binomial distributions fitted to the multiplicity distributions in various rapidity intervals $2 \cdot \Delta y$ centred around zero cms rapidity as a function of the hadronic cms energy W, (a) $\bar{n}$, (b) $1/k$.

4. The parameter $1/k$ for the full rapidity range as a function of W for this experiment (circles) and for meson – proton (Mp) scattering (squares) of ref. [3]. The dashed line is a fit to the $\bar{p}p$ and pp data [1] , the solid line is a fit to the e^+e^- data [3].

5. The parameters (a) $\bar{n}$ and (b) $1/k$ as a function of W for the full forward ($y > 0$, circles) and the full backward ($y < 0$, squares) μp hemispheres. The straight line shows $1/k$ for one e^+e^- hemisphere determined from $1/k$ for full e^+e^- events (solid line in Fig. 4) under the assumption that the two e^+e^- hemispheres are uncorrelated.

6. The parameters (a) $\bar{n}$ and (b) $1/k$ as a function of W for $y > 0.25$ ("forward", circles) and $y < 0.25$ ("backward", squares).

7. The parameter $1/k$ as a function of the width of the rapidity intervals extending (a) from $-\Delta y$ to $+\Delta y$, (b) from $y = 0$ to $-\Delta y$ in the backward hemisphere and (c) from $y = 0$ to $+\Delta y$ in the forward hemisphere, for selected intervals of W (in GeV).

8. The two – particle correlation function $C_2(y_1, y_2)$ vs. y_1 for the y_2 inter-

vals (a) -2<y_2<-1 , (b) -0.5<y_2<+0.5 , (c) 1<y_2<2 , for events in the energy range $12 < W < 20$ GeV.

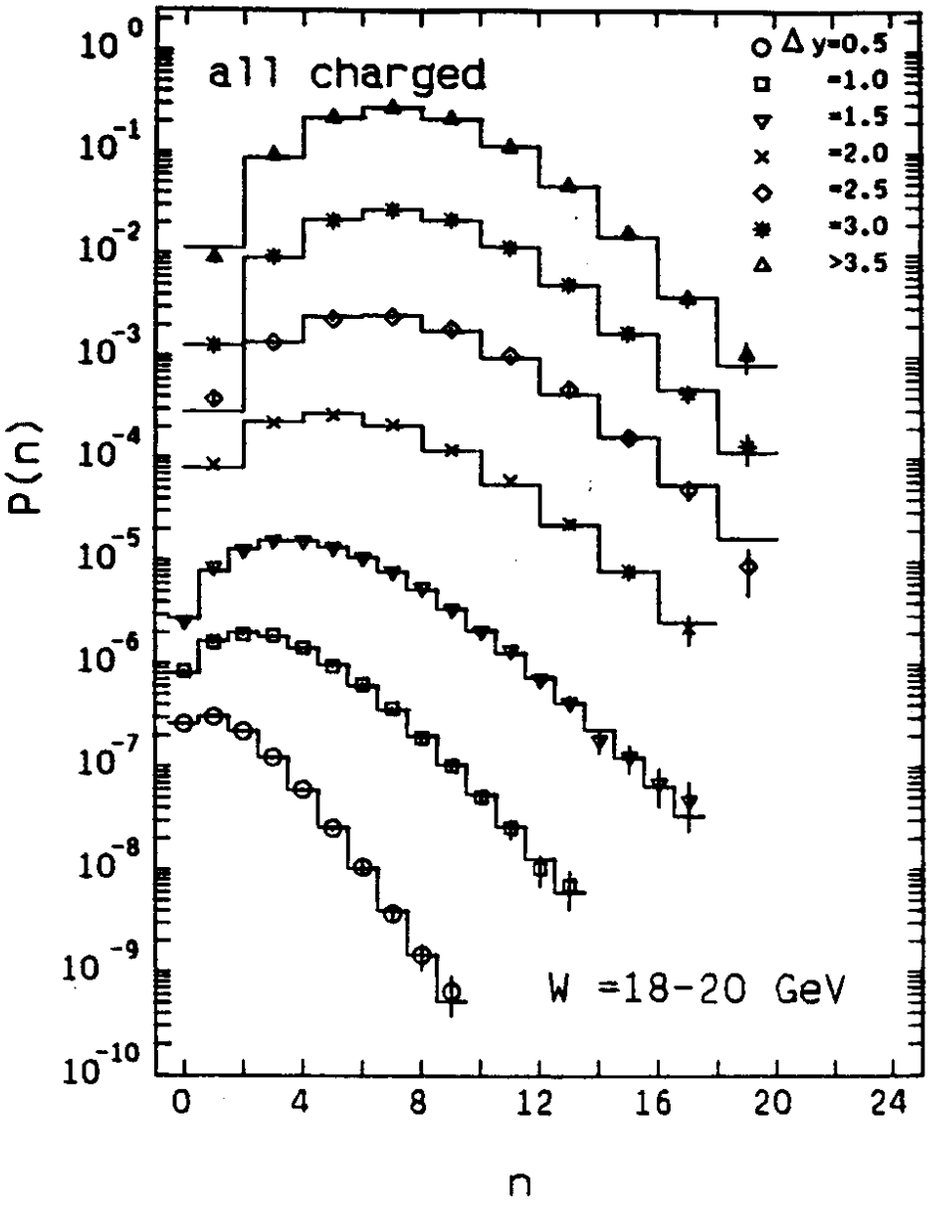
all charged
Δy=0.5
=1.0
=1.5
=2.0
=2.5
=3.0
>3.5
W =18-20 GeV
P(n)
n
10^0
10^-1
10^-2
10^-3
10^-4
10^-5
10^-6
10^-7
10^-8
10^-9
10^-10
0
4
8
12
16
20
24

Figure 1.

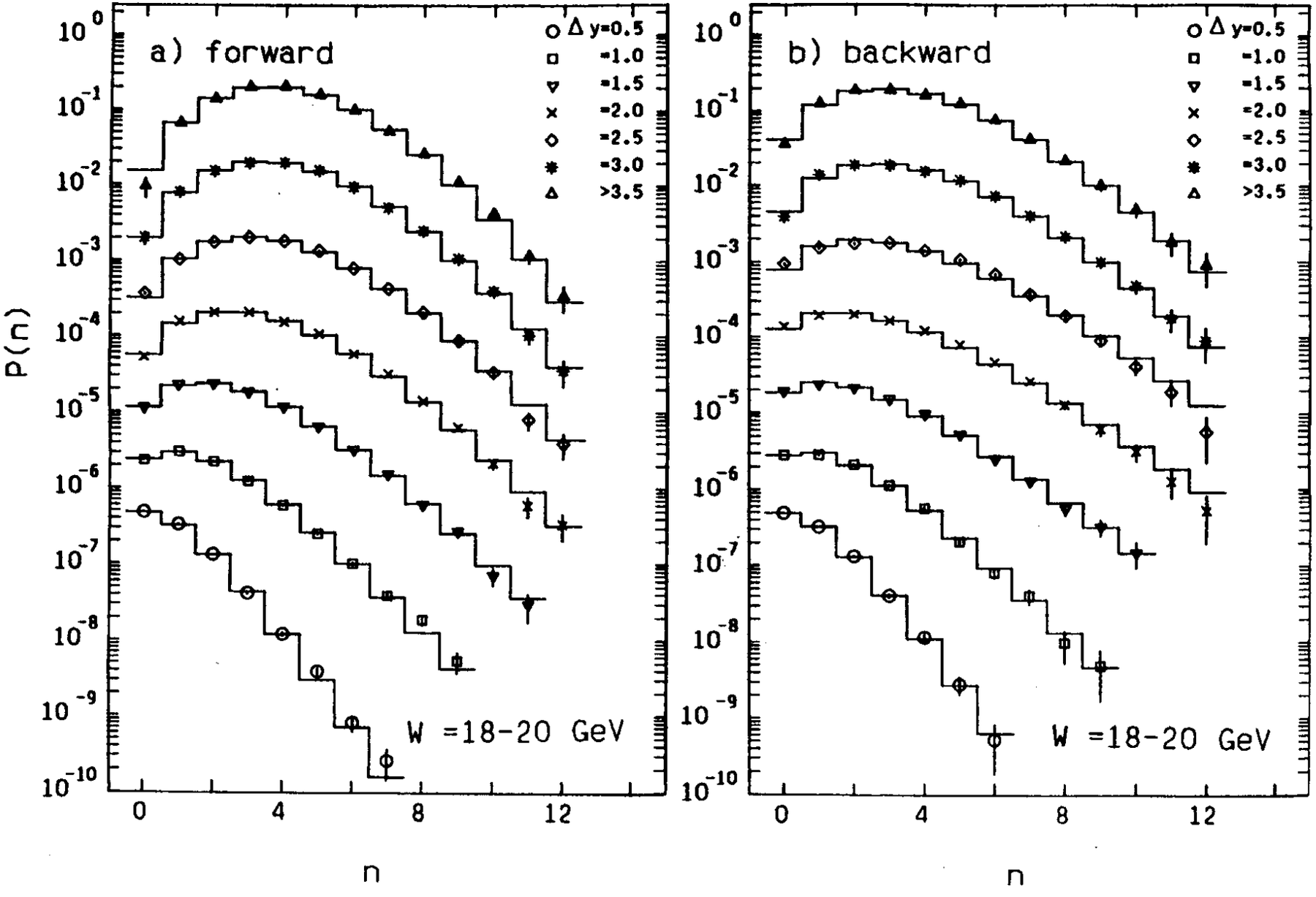

Figure 2.

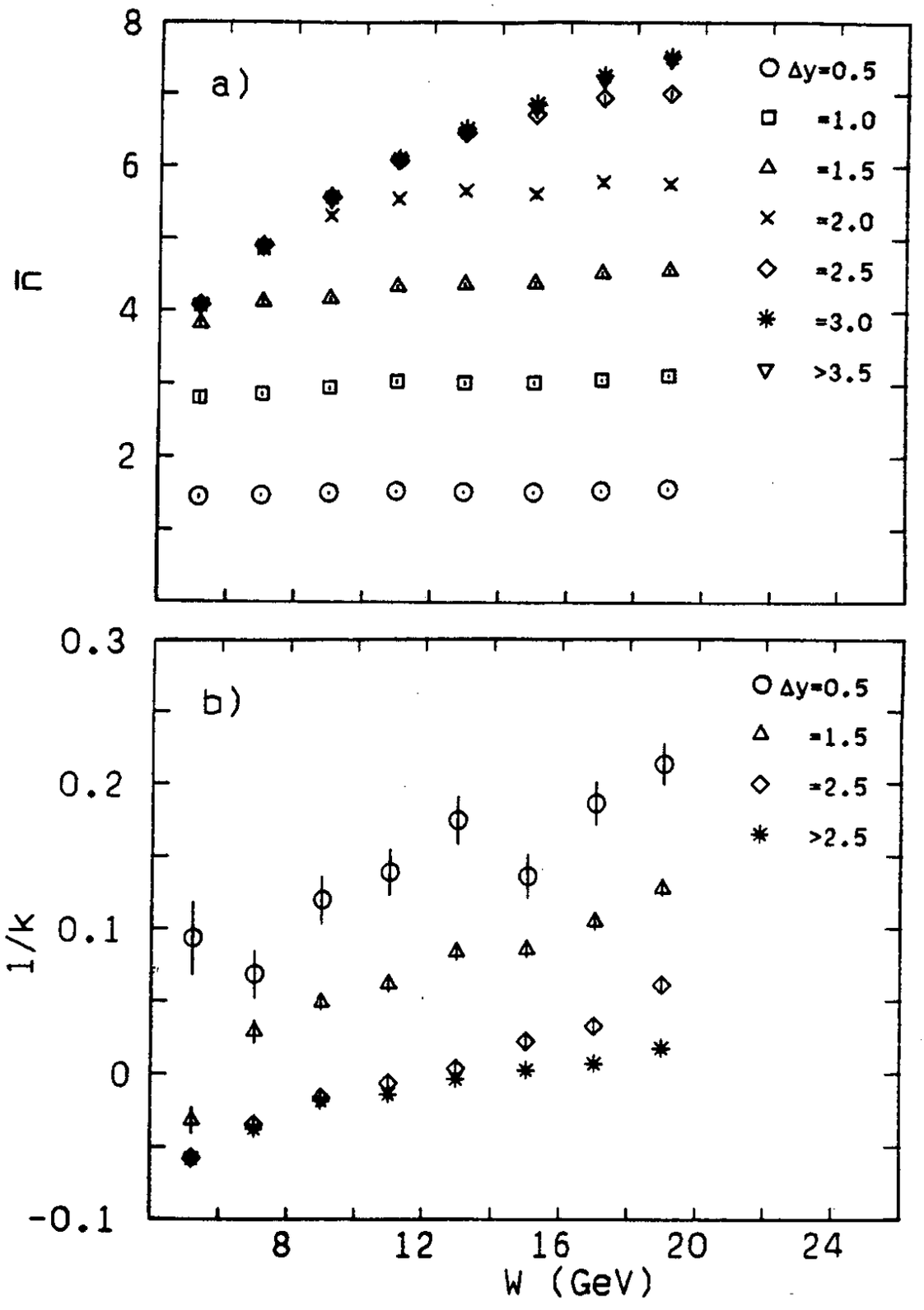
a)
Δy=0.5
=1.0
=1.5
=2.0
=2.5
=3.0
>3.5
C
8
6
4
2
b)
Δy=0.5
=1.5
=2.5
>2.5
1/k
0.3
0.2
0.1
0
-0.1
8
12
16
20
24
W (GeV)

Figure 3.

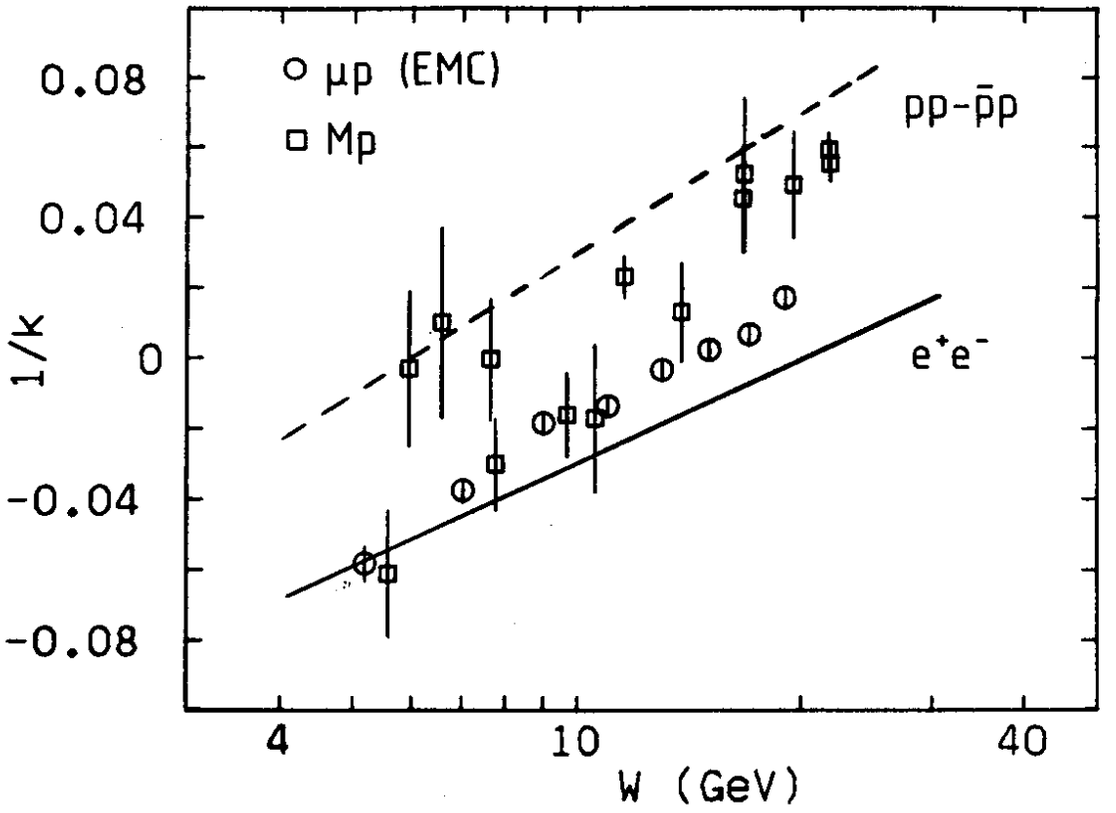

Figure 4.

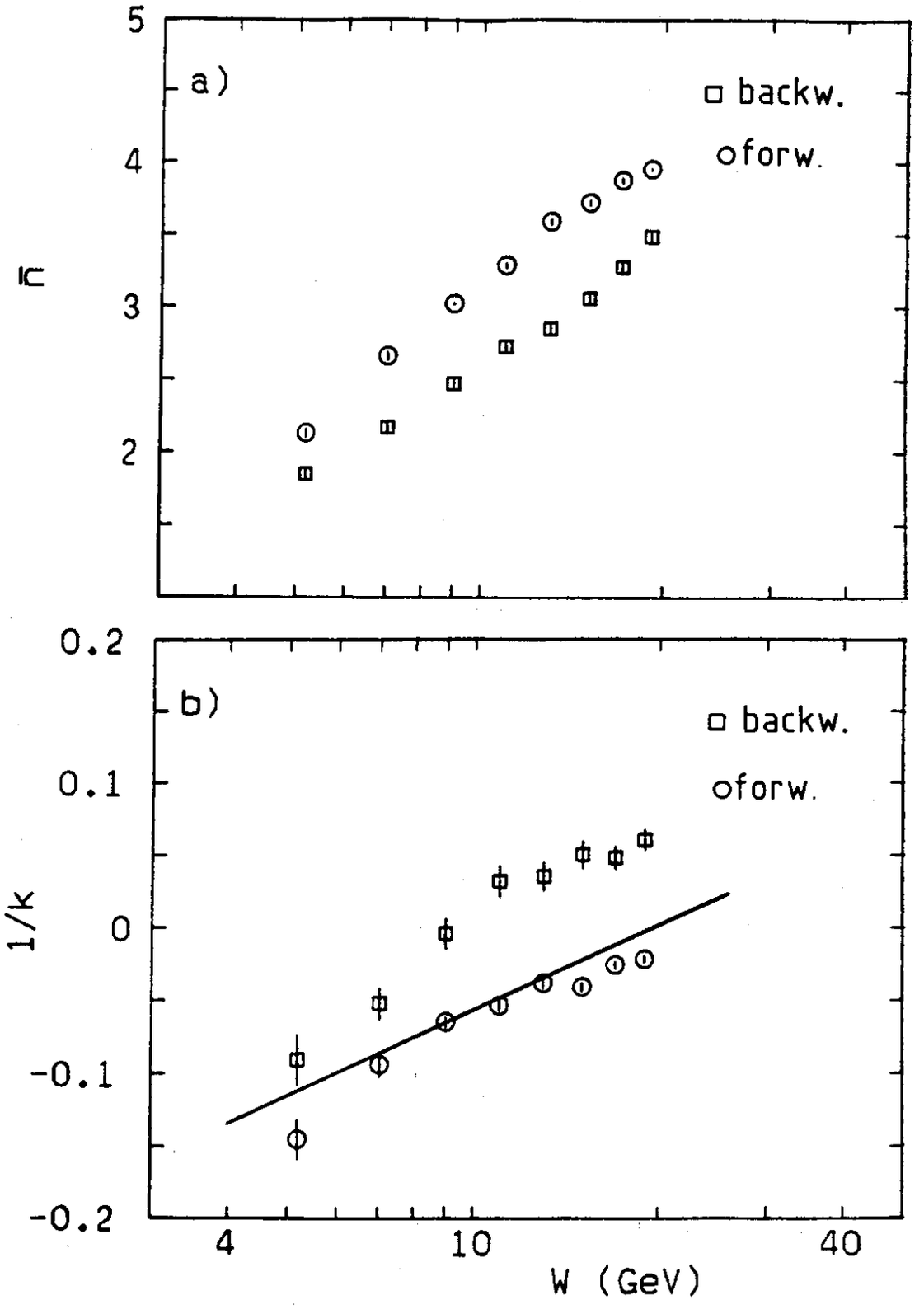

Figure 5.

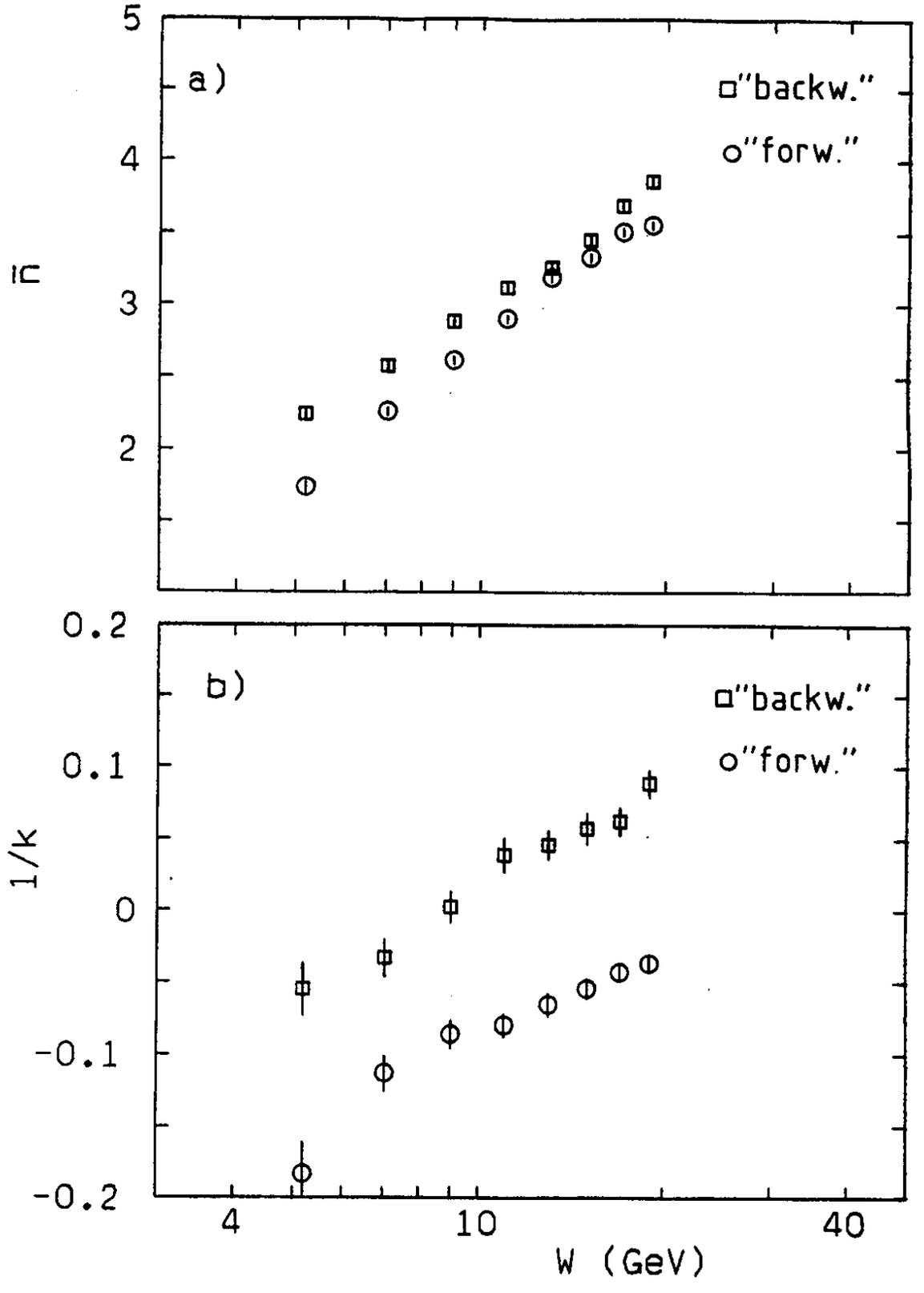

Figure 6.

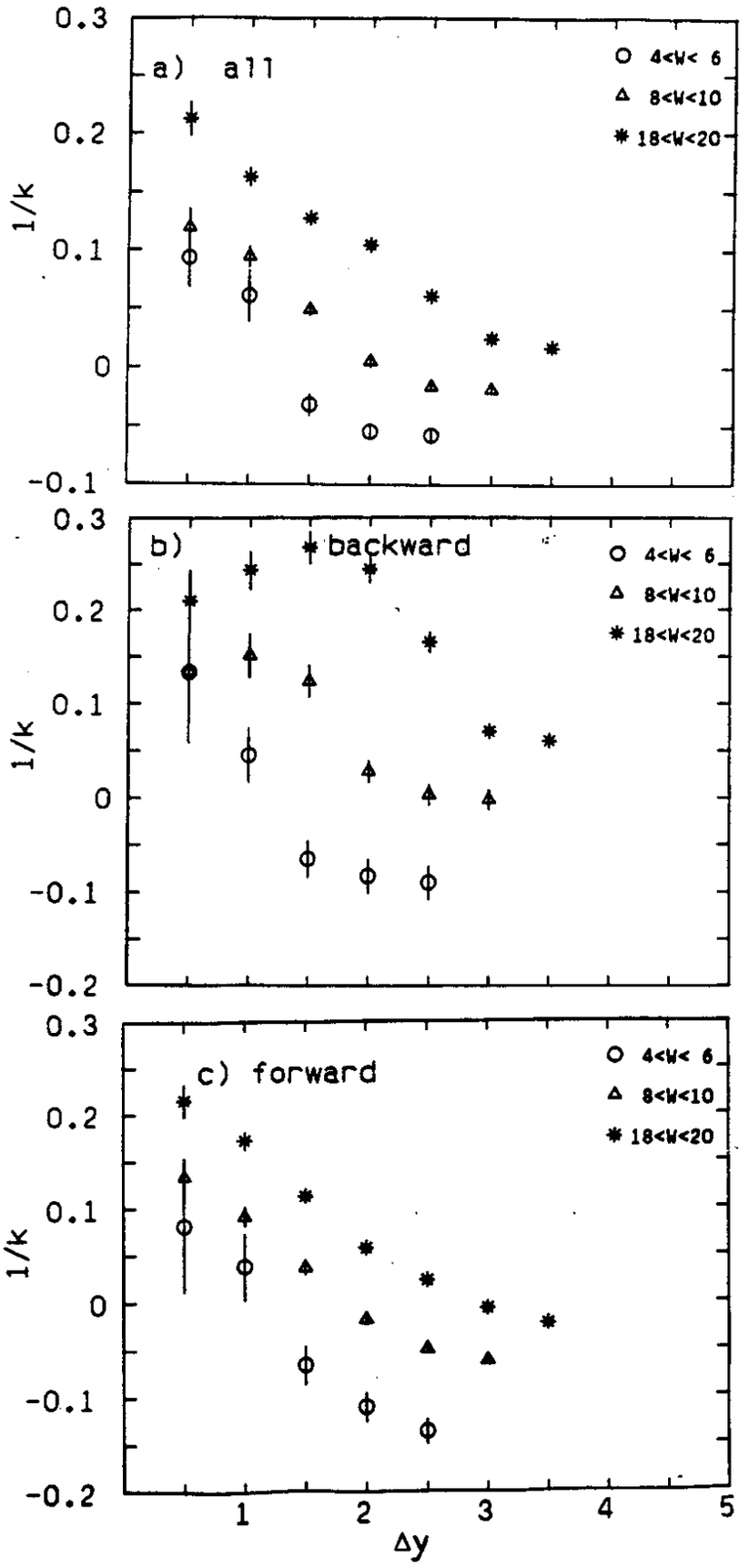
a) all
b) backward
c) forward
4<W< 6
8<W<10
18<W<20
1/k
Δy
0.3
0.2
0.1
0
-0.1
-0.2
1
2
3
4
5

Figure 7.

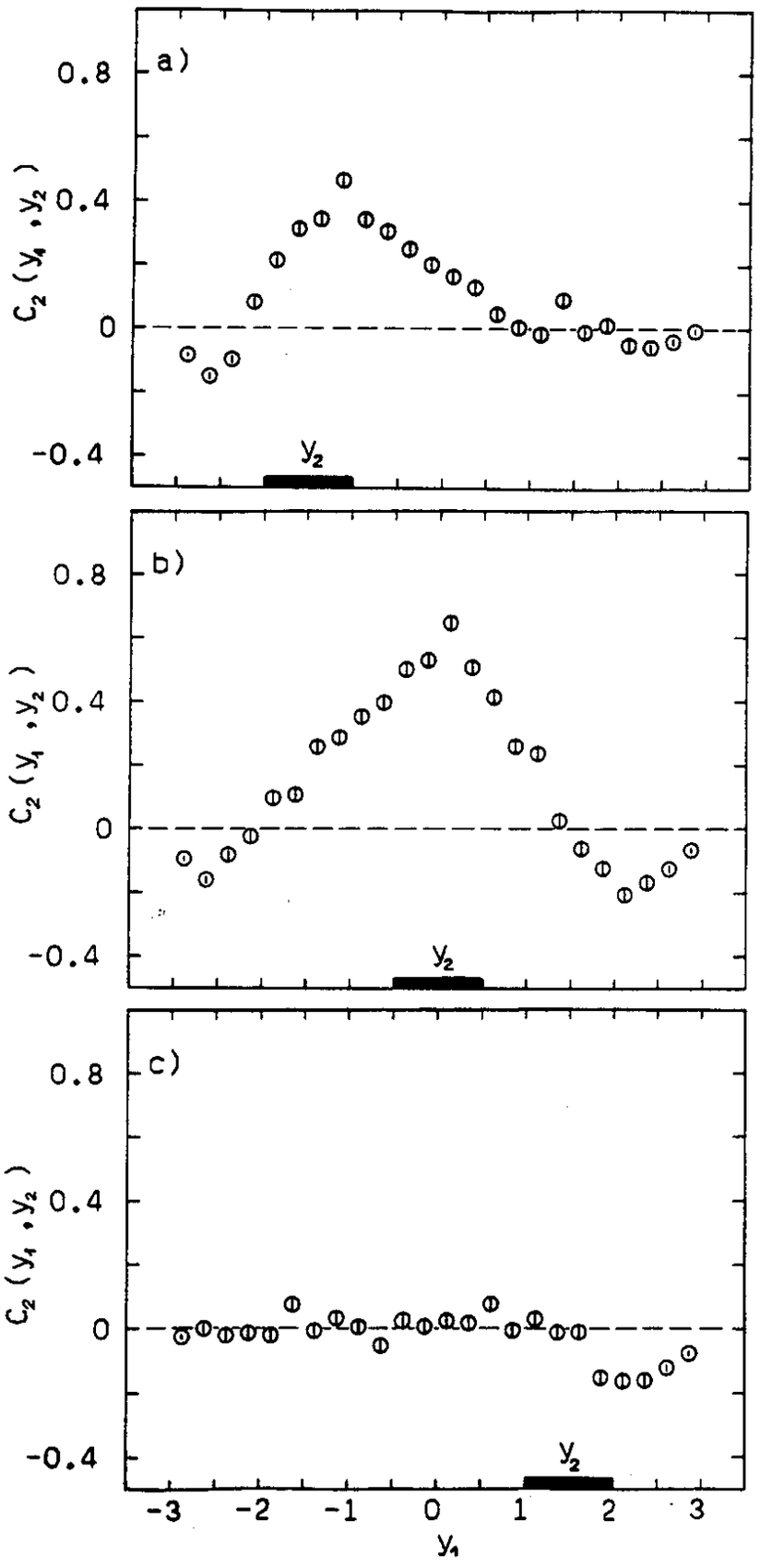

Figure 8.